Available online at www.sciencedirect.com

ScienceDirect

Procedia IUTAM 26 (2018) 124–131

Procedia IUTAM

www.elsevier.com/locate/procedia

IUTAM Symposium Wind Waves, 4–8 September 2017, London, UK

Wind modulation by variable roughness of ocean surface

Lev Ostrovsky[a,b]

[a]University of Colorado, Boulder, USA
[b]Institute of Applied Physics, Russian Acad. Sci., Nizhny Novgorod, Russia

Abstract

Recent results concerning transient effects of variation of short sea-surface wave roughness on near-surface turbulent wind are briefly outlined. This variation can be caused by oil, surfactants, inhomogeneous currents, internal waves, ship wakes, etc. To describe the wind parameters including surface stress and turbulent energy density, we use a direct solution of the Reynolds-type equations in the boundary-layer approximation. The solutions include a sharp and smooth roughness variation, 2-D surface variation, and a moving slick. The applicability of the theory was verified by comparison with laboratory data. Further on, the theory was applied to a problem related to the devastating tsunami near Fukushima Daichi in 2011.

Peer-review under responsibility of the scientific committee of the IUTAM Symposium Wind Waves.

Keywords: Wind modulation; Sea surface roughness; Reynolds equations;

1. Introduction

The interaction between wind and sea surface is a classic problem of ocean/atmosphere dynamics. The parameters of the wind flow, such as momentum flux and wind drag, are being thoroughly studied, mainly in terms of values averaged over the considered area. Wind variations over curved surfaces (hills, long waves) were also studied in detail, see, e.g., [1]. Transient problems considered in meteorology are generally focused on sharp changes in the underlying terrain; for example, a transition from water surface to shore or from field to forested land (e.g., [2]). Less studied are near-surface wind variations over horizontally varying sea roughness which are of importance in many practical cases, e.g., for evaluation of wind drift of oil spills and tsunami-caused debris, remote sensing of marine slicks, and others.

Methodically, most of the studies of horizontal wind variations were based on the two-layer approach (see [1–3] and references therein). Here we briefly outline the results based on direct solutions of the Reynolds-type equations for wind velocity and turbulent kinetic energy (TKE) simplified for the low boundary layer conditions. This theory, partially described in [3], allows to significantly extend the applications of the model, for example, to consider a smooth variation of roughness, moving inhomogeneities, two-dimensional “spots”, etc. In some cases the theoretical

2210-9838
Peer-review under responsibility of the scientific committee of the IUTAM Symposium Wind Waves.
10.1016/j.piutam.2018.03.012

results are applied to the data of a laboratory experiment and to modeling of wind over the debris floating from the Fukushima tsunami.

2. Basic equations

The general configuration of the considered process is shown in figure 1.

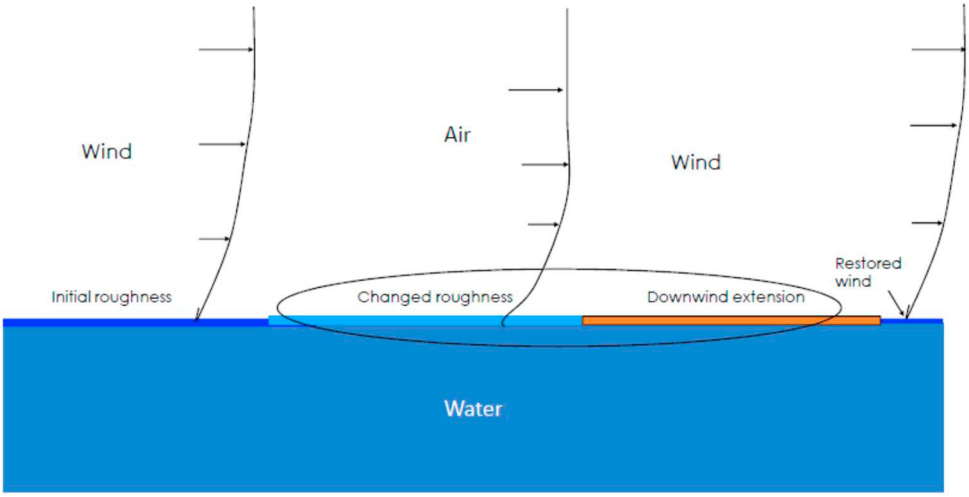

Fig. 1. Schematic of the wind variation over a finite area (spot) of changed roughness. The near-surface air flow changes over the spot and this variation can extend beyond the spot.

The starting point is Reynolds equations for an incompressible turbulent flow with neutral stratification [4, 5]:

$$\frac{\partial u_i}{\partial t}+(\mathbf{u}\cdot\nabla)u_i=-\frac{\partial p}{\partial x_i}-\frac{\partial \tau_{ij}}{\partial x_j},\ \tau_{ij}=-K\left(\frac{\partial u_i}{\partial x_k}+\frac{\partial u_k}{\partial x_i}\right),$$
$$\frac{\partial b}{\partial t}+(\mathbf{u}\cdot\nabla)b=\frac{\partial}{\partial x_i}\left[\kappa_b K\frac{\partial b}{\partial x_i}\right]+K\left(\frac{\partial u_i}{\partial x_k}+\frac{\partial u_k}{\partial x_i}\right)\frac{\partial u_i}{\partial x_k}-K\frac{\gamma b}{l_z^2},\qquad(1)$$
$$\nabla\cdot\mathbf{u}=0.$$

Here **u** is the average air velocity vector, p is pressure, b is the turbulent energy density (TKE), and τ_{ij} is the turbulent stress tensor. The parameters are: K is the turbulent exchange (viscosity) coefficient. In the framework of the Kolmogorov's eddy-viscosity closure hypothesis, $K=l_z\sqrt{b}$, l_z being the vertical turbulence scale, and the empirical coefficients are taken as $\kappa_b=0.7$ and $\gamma=0.05$ to 0.09 in different realizations. In what follows we use the boundary-layer approximation, letting $\partial/\partial x<<\partial/\partial z$ and $w<<u$, where u and w are the horizontal and vertical velocity components, respectively. Thus, the equations to be studied here are reduced to

$$\frac{\partial u}{\partial t}+u\frac{\partial u}{\partial x}+w\frac{\partial u}{\partial z}=\frac{\partial}{\partial z}\left(K\frac{\partial u}{\partial z}\right),$$
$$\frac{\partial u}{\partial x}+\frac{\partial w}{\partial z}=0, \tag{2}$$
$$\frac{\partial b}{\partial t}+u\frac{\partial b}{\partial x}=\kappa_b\frac{\partial}{\partial z}\left(K\frac{\partial b}{\partial z}\right)+K\left(\frac{\partial u}{\partial z}\right)^2-\frac{\gamma b}{l_z^2}.$$

For the stationary, horizontally homogeneous boundary layer above the surface, the solution of Eqs. (2) is the classic "law of the wall" logarithmic profile, which in standard notations is given by

$$u(z)=\frac{u_*}{\kappa}\ln\left(\frac{z}{z_0}\right), \tag{3}$$

with

$$b=b_0=\frac{u_*^2}{\gamma^{1/2}},\ l_z=\gamma^{1/4}\kappa z,\ \tau_{xz}=\tau_0=u_*^2. \tag{4}$$

Here $u(z)$ is the horizontal wind speed at the height z above the surface, u_* is the friction velocity, z_0 is the surface roughness scale, and $\kappa\approx 0.4$ is the dimensionless von Karman constant.

Another important parameter, stress, that is the vertical flux of horizontal momentum per unit mass, is

$$\tau_{xz}=S=l_z\sqrt{b}\frac{\partial u}{\partial z}, \tag{5}$$

and in the non-perturbed flow (3), $S=S_0=u_*^2$.

Evidently, Eqs. (2) and (3) cannot be directly used for modeling the horizontally inhomogeneous air flow considered here. In this case a non-trivial problem is to formulate boundary conditions for Eqs. (2) for a given roughness height $z_0(x)$. Since the general solution is not necessarily logarithmic, the parameters u_* and z_0 in the undisturbed solution, Eqs. (3) and (4), do not describe the transient processes. Thus, we assume that close to the surface at small heights $0 < z < z_1$ the new local logarithmic boundary layer has been quickly established. If $z_0(x, t)$ and $u_{*1}(x,t)$ for this new air flow profile are given, we define boundary conditions at $z = z_1$ as

$$u(z_1,x,t)=\frac{u_{*1}(x,t)}{\kappa}\ln\left(\frac{z_1}{z_0(x,t)}\right),\ b(z_1,x,t)=\frac{u_{*1}^2(x,t)}{\gamma^{1/2}},\ z_0<z_1. \tag{6}$$

These two expressions relate the values at $z = z_1$ with the surface roughness $z_0(x, t)$. In addition, this approach allows to avoid the description of a possible complex structure of turbulence near the surface. [1, 6] At a sufficiently large height, $z = h$, the wind flow is assumed to remain unchanged at the considered distances and time intervals, so that it retains the initial values, described by Eqs. (3) and (4). For control purposes, we performed calculations for different values of h while keeping other parameters fixed. In our case, $z_0 << z_1 << h$. We also suppose that the turbulence scale l_z remains linearly increasing with z, which is justified by the slowness of horizontal variations of all parameters as compared with vertical changes of the boundary layer profile. In what follows we consider different roughness spot geometries.

3. A slick

Consider a "slick spot" decreasing the roughness z_0 from 0.2 mm to 0.11 mm at a finite interval of x of 400 m length, possibly due to the surfactants. According to the above, a new logarithmic velocity profile is supposed to be formed below $z_1 = 4$ mm so that the velocity profile is given for $z = 4$ mm as shown in Fig. 2. The corresponding unperturbed wind velocity extrapolated to z = 10 m is 10.9 m/s.

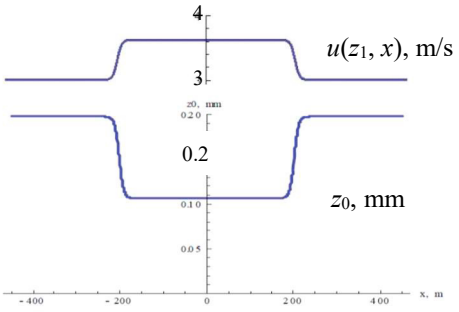

Fig. 2. Variation of surface roughness scale z_0 over a slick and the corresponding variation of wind speed at $z_1 = 4$ mm. The values of u are assumed unchanged from the initial logarithmic profile at at $x < -800$ m and at $z > 4$ m.

The results of calculation of variation of stress and turbulent energy using equations (2) are shown in figure 3.

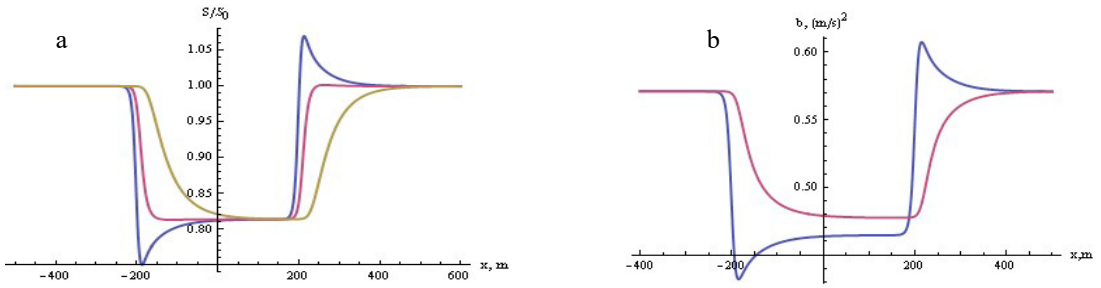

Fig. 3. (a) Relative variation of stress along the x axis at the heights of $z = 4$ mm (blue), 0.5 m (purple), and 2.95 m (olive). $S_0 = 0.16$ m^2/s^2 is an unperturbed value of S. (b) Variation of turbulent energy at the heights of $z = 2$ cm (blue) and 1 m (purple).

It is seen that the air flow characteristics are significantly changed over the slick. It is noteworthy that perturbations are shifted downwind so that a "precursor" perturbation is generated in front of the spot.

As mentioned, equations (2) allow to describe wind flow over a smoothly varying roughness, such as the one created by a surfactant of varying thickness or by a strong internal wave acting on the short surface waves. As an example consider the case when the initial wind's parameters are the same as in the previous example and the variation of velocity near the surface has the form

$$u(z_1 = 4 \text{ mm}) = 3.01 + 0.62 \exp(-x^2 / 150^2) \text{ m/s}. \quad (7)$$

This distribution and the corresponding roughness variation are shown in figures 4a,b. Figure 4c shows the resulting variation of stress at different levels.

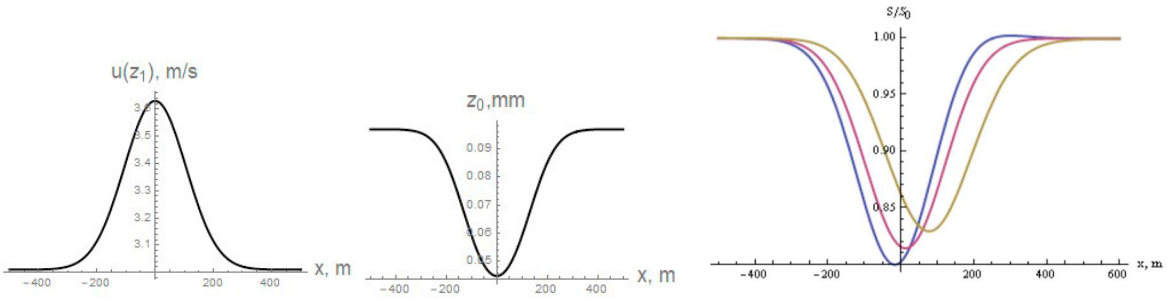

Fig.4. (a) Distribution of air velocity at z = 4 mm. (b) Variation of surface roughness, $z_0(x)$. (c) Variation of stress at z = 4 mm (blue), 0.5 m (purple) and 2.95 m (olive). Wind velocity at z = 10 m is 10 m/s.

Here again the perturbation is shifted ahead of the spot, especially at larger heights where the stronger wind carries the perturbation forward.

4. Moving spot

In general, system (2) can describe non-steady processes when the roughness varies in time. Fig. 5 gives an example of a perturbation moving with the velocity V as a result of, for example, action of a long wave or a ship changing surface roughness. In this case the left-hand parts of (2) have the form of $(u-V)\partial/\partial x$.

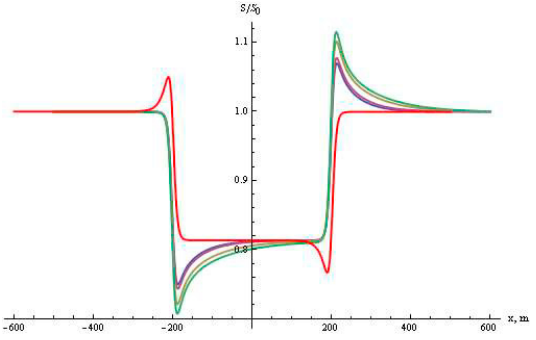

Fig. 5. Relative stress variation along the x axis at z = 4 mm at the upwind motions of the slick with velocities from V = 0 (green line), -1 m/s (olive), -5 m/s (purple), and -8 m/s (blue); and at the downwind motion with the velocity of 10 m/s (red). Other parameters are the same as in Fig. 3.

Here, for a steady upwind motion, stress profiles do not radically differ for a moving slick. However, the downwind curve is "inverted" to produce a “precursor” behind the spot. This indicates one important factor existing for the downwind motion: there can be a *synchronism* between the velocities of air and body at some height $z = z_s$. Thus, to satisfy causality, the wind should be given on the right of the spot at $z < z_s$ and on the left at $z > z_s$, and the solutions in these two areas should be matched. In figure 5 the case V = 10 m/s is shown for which $V > u(z)$ throughout the considered layer, z < 4 m, (indeed, at z = 4 m, wind velocity is 8.92 m/s) so that no singularities exist. For smaller V or for a thicker air layer, the point $u = V$ would be included. This "synchronous" case deserves a special consideration.

5. Finite-area spot

Consider now the case when the roughness area is bounded in all directions. In this case the wind perturbations are three-dimensional. The incident wind flow is still directed along the x-axis. One example is a smooth, two-dimensional variation of the velocity at $z = z_1$:

$$u(z_1 = 4\text{ mm}) = 3.01 + 0.66\exp\left(-x^2/150^2 - y^2/40^2\right)\text{ m/s}. \quad (8)$$

The solution of equations (1) for stress and turbulent energy are shown in figure 6.

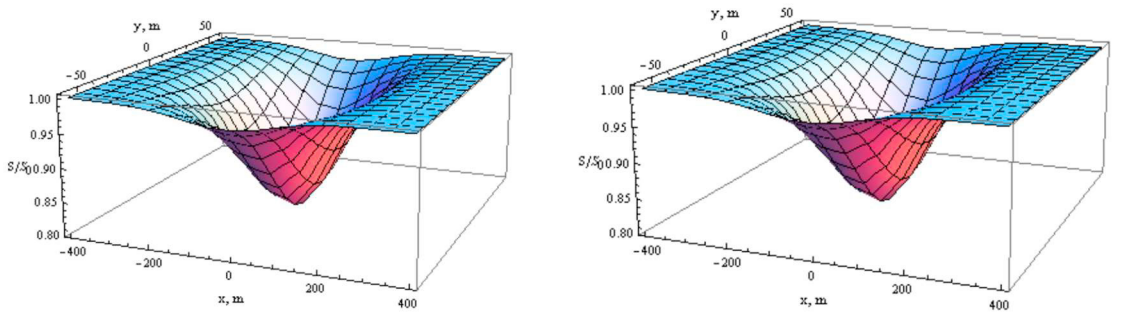

Fig. 6. 3D plots of (a) Variation of stress at z = 4 mm, (b) Variation of TKE at z = 2 cm. Incident wind parameters are the same as in Fig. 4.

Comparison with Fig. 4 shows that the order of variation of wind parameters is the same as in the 2D case. Note, however, that in the 3D case there appears a shear in wind over the spot which can result in instabilities and generation of vortex motions.

6. Comparison with laboratory experiment

In [3] a relevant laboratory experiment (carried out by S. Ermakov and O. Shomina at the Institute of Applied Physics of Russian Acad. Sci.) in a wind-wave tank is described. The tank is a closed channel with a rectangular water cross-section 30 x 30 cm^2 and a 30 x 30 cm^2 air channel above it. The wind over water was produced by a frequency-controlled fan. The water surface roughness was changed by dropping a surfactant (oleic oil) on the water surface. When the dropper worked for a finite time period, a slick was formed, and the wind parameters over the slick were measured. Figure 7 shows the data for one realization. It is seen that the theory yields correct ranges of wind velocity variation over the film at different heights; it also predicts the observed transient areas both in the beginning and at the end of the process, as well as the extension of wind perturbation beyond the roughness variation shown in Fig. 7a.

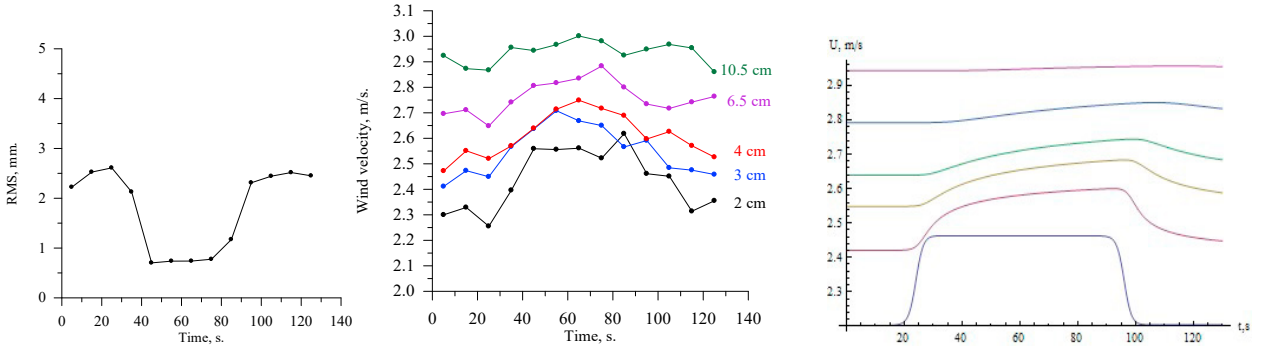

Fig. 7. Wind speed variation over a slick in laboratory tank (a) R.m.s of wind wave height over a film drifting past the wire gauge during about 80 s. (b) Wind velocities at different heights over the water surface, measured by a hot wire anemometer. (c) Theoretical modelling according to the above theory. Theoretical curves are plotted for the same heights (2, 3, 4, 6.5, and 10.5 cm). as the experimental ones, except for the lower one showing the boundary condition at z_1 = 1 cm; the latter was taken from the measured wind profile.

7. Wind variation over floating debris

The approach described above was recently used in [7] for evaluation of early interaction between wind and debris floating after the devastating tsunami having destroyed the Fukushima Daiichi nuclear power station in Japan. On retreating, the tsunami carried oil, loose debris, and wreckage seaward (estimated 5 million tons) which suppresses the surface waves as was confirmed by radar measurements from a SAR satellite. This, according to our estimates, the wind speed increases over the surface and, as a result, provides an additional (of the order of 5 cm/s) acceleration of floating debris against the velocities expected from a current-related drift and an unchanged wind. Figure 8 illustrates some of these results.

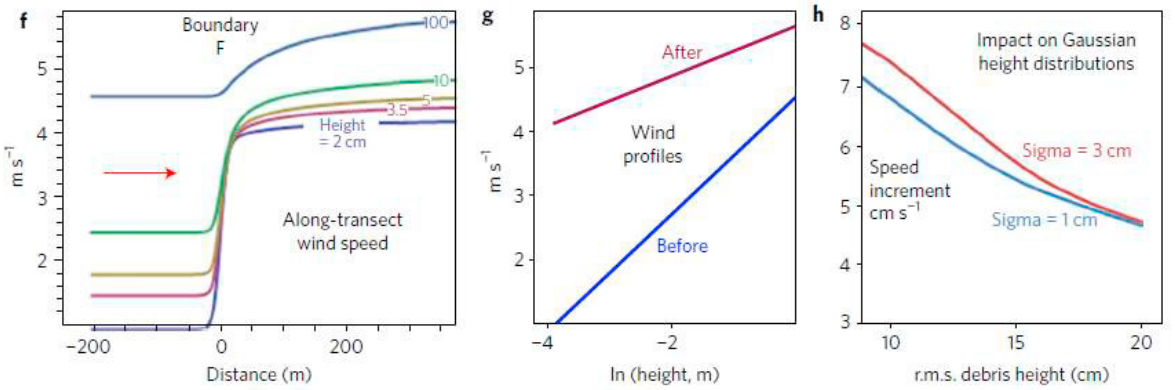

Fig. 8. (f) Wind velocity variation on the path through the slick at heights of 2–100 cm calculated based on Eqs. 2. (g) Calculated logarithmic wind profile before and after crossing the slick edge. (h) Estimated drift speed increments due to wind restructuring for idealized floating debris (6.2m/s local wind at $z = 10$ m). From [7].

As in the above examples, the wind speed increases over the slick, and after crossing the slick edge a new logarithmic wind profile is eventually formed (Fig. 8g). The enhanced wind, in its turn, accelerates the floating products as follows from independent calculations, see Fig. 8h. These results are in agreement with the measured data.

8. Conclusions

Here the theory of turbulent air flow over a variable sea roughness with using the semi-empirical Reynolds-type equations and simple closure hypotheses has been developed. This theory which does not involve dividing the atmospheric boundary layer to two or more areas looks quite adequate for low heights where the wind most intensively interacts with the waves. It should be noted that for stationary surface inhomogeneities this approach gives the results close to those following from the two-layer consideration [3]. However, the present approach is applicable for more general configurations, such as smooth inhomogeneities, moving slicks, and two-dimensional inhomogeneities. The theory is confirmed by laboratory experiment and it was successfully applied to description of a real tsunami event. Note that effect of the areas of intensified roughness ("suloys") can also be described by the used equations. Note also that although in general equations (2) include the effect of vertical air motion, in many cases it can be neglected which further simplifies the solution; however, it has to be verified in each specific case.

Even in the framework of the simplified approach considered above, there remain interesting unsolved problems. One is, as mentioned, the synchronism between the moving spot velocity V and wind velocity $u(z)$ at some height if the latter is located at some $z = z_c$ within the considered air layer. In this case the boundary condition for x should be prescribed on the right at $z < z_c$ and on the left at $z > z_c$ and the solutions should be matched at $z = z_c$. Another interesting problem is a reciprocal effect: reaction of the surface on the changes of the surface stress due to

wind modification. Our preliminary evaluations of this effect based on the Charnock's formula [8] indicate a possibility of positive feedback when the effect cumulates.

Acknowledgements

Selected results of the recent publications [3] and [7] have been used here, and the author is grateful to the co-authors of these works. Special thanks are to M. Charnotskii for the longtime and fruitful collaboration,

References

1.S. E. Belcher, J. C. R. Hunt, Turbulent flow over hills and waves, *Ann. Rev. Fluid Mech.*, 1998; **30:** 507-5380.
2. S. A. Savelyev, P. A. Taylor, Internal boundary layers: I. Height formulae for neutral and diabatic flows, *Boundary-Layer Meteorology*, 2005; **115**:1-25.
3. M. Charnotskii, S. Ermakov, L. Ostrovsky, O. Shomina, Effect of film slicks on near-surface wind, *Dyn. Atm. Oceans*, 2016; **75**:118-128.
4.A. S. Monin, A. M. Yaglom, (1973) *Statistical Fluid Mechanics - Vol. 1: Mechanics of Turbulence*, 1973; MIT Press, Boston, 782 pp.
5.C. G. Speziale, Analytical methods for the development of Reynolds-stress closures in turbulence, *Ann. Rev Fluid Mech*.,1991; **23**:107-157.
6. O. A. Druzhinin, L. A. Ostrovsky, Dynamics of turbulence under the effect of stratification
and internal waves, *Nonlin. Proc. Geophys*., 2015; **22:** 337–348.
7. J. Matthews, L. Ostrovsky, Y. Yoshikawa, S. Komori, H. Tamura, Dynamics and early post-tsunami evolution of floating marine debris near Fukushima Daichi, *Nature Geoscience*, 2017; DOI:10.1038/NGEO2975.
8. H. Charnock, Wind stress on a water surface, *Quart. J. R. Met. Soc*., 1955; **81:** 639-640.